Electrochimica Acta 180 (2015) 409–418

Contents lists available at ScienceDirect

Electrochimica Acta

journal homepage: www.elsevier.com/locate/electacta

Enhanced Electrochemiluminescence of *N*-(aminobutyl)-*N*-(ethylisoluminol) Functionalized Gold Nanoparticles by Graphene Oxide Nanoribbons

Nur Syakimah Ismail[a,b], Quynh Hoa Le[a], Quamrul Hasan[c], Hiroyuki Yoshikawa[a], Masato Saito[a], Eiichi Tamiya[a,*]

[a] Department of Applied Physics, Graduate School of Engineering, Osaka University, 2-1 Yamadaoka, Suita, Osaka 565-0871, Japan
[b] School of Microelectronic Engineering, Universiti Malaysia Perlis, Kampus Pauh Putra, 02600 Arau, Perlis, Malaysia
[c] School of Technology Management and Logistics, UUM College of Business, Universiti Utara Malaysia, 06010 Sintok, Kedah, Malaysia

ARTICLE INFO

Article history:
Received 31 May 2015
Received in revised form 7 August 2015
Accepted 11 August 2015
Available online 28 August 2015

Keywords:
electrochemiluminescence
isoluminol
graphene oxide nanoribbon
gold nanoparticle
screen-printed electrode

ABSTRACT

The mechanism of electrochemiluminescence (ECL) of an *N*-(aminobutyl)-*N*-(ethylisoluminol) -functionalized gold nanoparticle (ABEI-AuNP) hybrid with graphene oxide nanoribbons (GONRs) as a functional supporting matrix on a modified screen-printed electrode (SPE) was studied under alkaline conditions. In our catalytic system, ABEI-AuNPs supported by GONRs were profoundly superior to the unsupported ABEI-AuNP/SPE, and exhibited greatly enhanced ECL intensity (≈30.0%). This difference is attributed not only to an 80.2% increase in the total surface area of the ABEI-AuNP-GONR/SPE, but also to enhancements of the ABEI-AuNP catalytic activity resulting from metal-oxygen bonding between the functional groups on the GONRs and the Au active sites. This improved catalytic activity of ABEI-AuNP facilitates both oxidative radical generation and fast reaction kinetics of the ABEI oxidation process. To further elucidate the mechanism of the counter-peak phenomenon in the ABEI ECL under cyclic voltammetry (CV) conditions, the effects of various factors, including pH of buffer solution, existence of dissolved oxygen, and concentration of hydrogen peroxide, on the ECL of ABEI were investigated. The mechanisms of liquid-phase ABEI on bare SPE and GONR/SPE were also compared to that of solid-phase ABEI-AuNP to validate the proposed mechanism for ABEI-AuNP-GONR/SPE.

1. Introduction

Electrochemiluminescence or electrogenerated luminescence (ECL) has become an important detection method in analytical chemistry because of its simplicity, rapidity and high sensitivity [1,2]. Luminol (3-amino-phthalhydrazide) is the most widely used ECL reagent, and the decomposition of luminol results in the production of excited states (3-amino-phthalate, 3-AP*) and the emission of blue light through an annihilation process [3]. Many studies have been devoted to understand the mechanism of luminol ECL in the luminol-hydrogen peroxide (H_2O_2) system [4–6]. Because H_2O_2 plays an important role in generating oxygen-related radicals for that interact with the luminol radical, two main issues were chiefly focused upon when identifying the appropriate catalyst. First, a peroxidase- or oxidase-based enzyme was utilized to catalyze the production of H_2O_2 [7,8], and second, a noble metal was used to accelerate the generation of oxygen-related radicals to achieve rapid and enhanced ECL intensity [9,10]. Previous research has revealed that the behavior of luminol ECL is highly dependent on the pH of the buffer solution, and is facilitated by alkaline conditions, although enzyme activity is present only under neutral conditions [11]. Moreover, the enzyme has several major drawbacks, including its high cost, sensitivity to temperature, and complex requirements for binding on the electrode surface [12]. In contrast, noble metal catalysts, especially gold (Au), are very reactive under alkaline conditions because hydroxide anions promote non-covalent interactions on metal active sites [13]. This phenomenon significantly enhances Au reactivity, making it compatible with luminol ECL. Furthermore, Au has been shown to enhance chemiluminescence (CL) and ECL activity, particularly in the nanoparticle form. However, the catalytic performance of gold nanoparticles (AuNPs) in luminol ECL was dependent on the

* Corresponding author at: Department of Applied Physics, Graduate School of Engineering, Osaka University, 2-1 Yamadaoka, Suita, Osaka 565-0871, Japan. Tel.: +81 6 6879 4087; fax: +81 6 6879 7840.
E-mail addresses: syakimah@unimap.edu.my (N.S. Ismail), lequynhhoa.env@gmail.com (Q.H. Le), quamrul@uum.edu.my (Q. Hasan), yosikawa@ap.eng.osaka-u.ac.jp (H. Yoshikawa), saitomasato@ap.eng.osaka-u.ac.jp (M. Saito), tamiya@ap.eng.osaka-u.ac.jp (E. Tamiya).

http://dx.doi.org/10.1016/j.electacta.2015.08.043
0013-4686/

particle size [14], nature of the support matrix [15], and the preparation method [16,17].

Recently, we reported that the catalytic activity of AuNPs was enhanced by using graphene oxide nanoribbons (GONRs) as a functional supporting matrix for a non-enzymatic glucose sensor [18]. Graphene is a single-atom-layer honeycomb lattice of carbon atoms in an sp^2 hexagonal bonding configuration, which is the basic building block of carbon materials [19]. An improved technique in chemically derived graphene is the longitudinal unzipping of CNTs to form GONR precursors using oxidizing agents in strongly acidic conditions [20]. Because of the strong oxidative reaction that occurs during the unzipping process, the resulting GONRs are highly soluble in water and polar solvents, and exhibit an attractive surface and edges containing oxygen functional groups [20,21]. The utilization of GONRs increased the total surface area of the AuNPs and resulted in three-dimensional specific interactions between the GONR functional groups and AuNP active sites containing the reactant and intermediates, thereby promoting the reaction kinetics [18]. However, the burst nucleation method used for producing AuNPs required the employment of hexane as a surfactant to avoid particle aggregation, which required a thermal treatment at 400 °C after electrode fabrication for removal. The thermal treatment step was necessary not only to activate the AuNP catalytic surface by removing the stabilizing agents but also to bind AuNPs on the GONRs to increase their stability [18]. However, our ECL setup makes use of a screen-printed electrode (SPE) comprising a glass epoxy substrate that cannot withstand high-temperature treatment [22]. Therefore, the synthesis of surfactant-free AuNPs is required.

Cui's group has reported the synthesis of AuNPs by using the luminol derivative *N*-(aminobutyl)-*N*-(ethylisoluminol) (ABEI) as a reducing agent through the seed growth method at room temperature [23]. This simple method is capable of coating ABEI on the surface of AuNPs without using a surfactant. As a result, this particle can emit light by itself in the absence of supplementary luminol in the solution, which makes it an attractive label, especially for immunosensors [24]. To the best of our knowledge, the catalytic performance of this particle has not been studied on any supporting matrix except the cysteine linker [25]. Herein, for the first time, we investigate the performance of ABEI-functionalized AuNPs hybridized with GONRs on a carbon SPE (ABEI-AuNP-GONR/SPE) for the ECL of ABEI under alkaline conditions. The catalytic performance of the ABEI-AuNP without the GONR supporting matrix on SPE was also studied. In addition, the ECL of ABEI in aqueous alkaline conditions on bare SPE and GONR-modified SPE was investigated to further elucidate the ECL mechanism of ABEI-AuNP-GONR/SPE. These interesting results obtained may provide an insight into the ECL mechanism of ABEI on a solid-liquid interface and facilitate further improvements of ECL sensors through the use of noble metals and GONRs as a functional supporting matrix. Furthermore, SPE has great potential for the development of portable, rapid, and sensitive biosensing devices.

2. Experimental

2.1. Materials and reagents

Multi-walled carbon nanotubes (MWCNTs), hydrogen tetrachloroaurate (III) tetrahydrate ($HAuCl_4{\cdot}4H_2O$), 0.1 M sodium hydroxide (NaOH), concentrated sulfuric acid (H_2SO_4), potassium permanganate ($KMnO_4$), 30% hydrogen peroxide (H_2O_2), ethanol and ether were obtained from Wako Co. (Japan). *N*-(4-Aminobutyl)-*N*-ethylisoluminol was purchased from Tokyo Chemical Industry Co. Ltd. (Japan). Carbonate buffer solution (CBS, 0.1 mol L^{-1}, pH 9.02–10.72) was prepared from Na_2CO_3 and $NaHCO_3$. Ultrapure water was obtained from Barnstead Nanopure Water Purification System (18 MΩ, Thermo Scientific, USA) and used throughout the experiments.

2.2. Electrode fabrication and characterization

2.2.1. Synthesis of GONRs

GONRs were synthesized through the longitudinal unzipping of MWCNTs [18,20]. Briefly, MWCNTs were suspended in concentrated H_2SO_4 for 12 h, and then treated with $KMnO_4$. The mixture was stirred at room temperature for 1 h, and then heated at 55–70 °C for a further 1 h. After all $KMnO_4$ had been consumed, the reaction was quenched by pouring the mixture into ice containing 1.25% H_2O_2. The solution was filtered through a polytetrafluoroethylene (PTFE) membrane. The remaining solid was washed with HCl and ethanol/ether alternately between filtrations. The final product was dried *in vacuo*.

2.2.2. Synthesis of ABEI-AuNP

AuNPs were synthesized through a seed-growth method using ABEI as the reducing agent [23]. First, stock solutions of $HAuCl_4{\cdot}4H_2O$ in water (5.9 mM) and ABEI in 0.1 M NaOH (4 mM) were prepared. Then, $HAuCl_4$ stock solution (9 mL) was mixed with water (45 mL). The ABEI stock solution (6 mL) was added rapidly while stirring. The reaction mixture was stirred at room temperature for 2 h. Subsequently, the $HAuCl_4$ stock solution (6 mL) was added, and the reaction mixture was continuously stirred for another 2 h. Finally, the mixture was dialyzed for 3 days, during which the water was changed frequently to remove the unreacted reagent. The produced ABEI-AuNPs were kept at 4 °C when not in use.

2.2.3. Fabrication of ABEI-AuNP and ABEI-AuNP-GONR-modified SPE electrodes

An SPE was used for all electrochemical measurements. The carbon-based SPE consist of a three-electrode system: a working electrode, counter electrode, and Ag/AgCl reference electrode. The working electrode area is 2.64 mm^2 and the total size including the connection part and the carbon barrier to prevent the solution from flowing into the connector is 12.5 mm × 4 mm × 0.3 mm [26]. A small volume of solution (20 μL) was applied directly onto the electrode surface and the SPE was discarded after a single use.

Surface modification of the SPE working electrode was achieved by the drop casting method. First, GONRs (1 mg) were sonicated and dispersed in 1 mL of water. Then, the mixture of as-prepared ABEI-AuNP and GONR was sonicated for 30 min. Finally, the mixture of ABEI-AuNP-GONR (2 μL) was cast on the SPE working electrode and dried at room temperature overnight. For comparison, ABEI-AuNP-modified SPE was prepared by the direct casting of as-prepared ABEI-AuNP (2 μL) onto the working electrode.

2.2.4. Characterization of ABEI-AuNP-GONR material and ECL measurement

The formation of AuNPs by reducing $HAuCl_4$ with ABEI was confirmed by UV–vis spectrophotometry (Shimadzu UV-2550, Japan). The functional groups on the ABEI-AuNPs and GONRs were confirmed by attenuated total reflectance–Fourier transform infrared (ATR-FTIR) spectroscopy (Horiba FT-720, Japan). The morphologies of the catalytic materials were acquired by scanning electron microscopy (SEM) using a DB 235 microscope (FEI Co.). All electrochemical measurements were performed with a USB-powered handheld potentiostat (BDTminiSTAT100; Biodevice Technology Co. Ltd., Japan) [27]. The ECL of ABEI was observed with an EM-CCD digital camera and recorded with AquaCosmos software, whereas the ECL intensity was measured by a photon detector unit (Hamamatsu Photonics, Japan).

3. Results and Discussions

3.1. Characterization and morphological inspection of ABEI-AuNP-GONR/SPE

The formation of ABEI-AuNP was confirmed by the UV–vis absorption spectra of ABEI and $HAuCl_4$ precursor before and after the reduction process as demonstrated in Fig. S1 (in Supporting Information). The characteristic absorption peak of pure ABEI appeared at 290 nm with a shoulder at 320 nm [23], and the $HAuCl_4$ absorption peak was observed at 290.5 nm. After stirring for 4 h, the mixture of ABEI and $HAuCl_4$ exhibited a peak shift to 298 nm and a shoulder shift to 350 nm with the appearance of a small peak at 525 nm indicating the formation of AuNPs. After 3 d of dialysis, the mixture showed a decrease in ABEI absorption peaks and an increase the characteristic Au spectrum. This result suggests that the concentration of ABEI was decreased after reaction with $HAuCl_4$ to form AuNPs. Moreover, the existence of both ABEI and AuNP peaks might indicate that the resultant AuNPs were coated with ABEI molecules because the dialysed supernatant removed other contaminant. The size of the as-prepared ABEI-AuNPs were confirmed to be ~38 nm (Fig. S2).

After confirming the formation of ABEI-AuNPs, the as-prepared ABEI-AuNPs and ABEI-AuNP-GONR composite were drop cast (2 μL) on the working electrode of the SPE. Fig. 1A presents an illustration of the ABEI-AuNP-GONR composite on the SPE working electrode. Additionally, Fig. 1B displays SEM images of the ABEI-AuNPs on the SPE (Fig. S3) with and without the GONR supporting matrix. The ABEI-AuNP-modified SPE (ABEI-AuNP/SPE) shows the aggregation of ABEI-AuNPs, forming a Au layer (Fig. 1B(i)). In contrast, the mixture of ABEI-AuNPs and GONRs produced a homogenous layer of ABEI-AuNP-GONR on the SPE (ABEI-AuNP-GONR/SPE), as depicted in Fig. 1B(ii). This result suggests that the oxygen functional groups on the GONRs might engage in electrostatic bonding with ABEI-AuNPs, thus hindering the aggregation process [28]. These functional groups in the GONR matrix are expected to play an important role in enhancing the catalytic activity of ABEI-AuNPs at the solid-liquid interface. Further characterizations of each catalytic material for the ECL of ABEI under alkaline conditions are presented in the following sections.

3.2. ECL of ABEI-AuNP-GONR-modified SPE

The general scheme of the ECL of the luminol-H_2O_2 system under alkaline conditions can be seen in Fig. 2 [1]. Luminol and H_2O_2 dissociate to form luminol monoanion (LH^-) and hydrogen peroxide anion (HOO^-), respectively. Then, HOO^- is oxidized to oxygen via the hydroperoxy radical $HOO^{\bullet -}$, while LH^- is oxidized to 3-amino-phthalate (3-AP) via the diazasemiquinone radical ($LH^{\bullet -}$) during the forward scan [29]. Subsequently, $LH^{\bullet -}$ reacts with the superoxide radical ($O_2^{\bullet -}$), which is produced through the dissociation of $HOO^{\bullet -}$ intermediates, to yield the hydroperoxy intermediate (LOO^-), which causes the excited state of 3-amino-phthalate (3-AP*) by releasing nitrogen. Then, 3-AP* returns to the ground state by emitting fluorescence [1,4,5,29]. To understand the ECL mechanism of ABEI on ABEI-AuNP-GONR/SPE, we performed cyclic voltammetry (CV) on each catalytic material separately, as depicted in Fig. 3. Initially, SPE and GONR-modified SPE (GONR/SPE) were tested in a 0.364 mM ABEI solution. The concentration of ABEI used to test the SPE and GONR/SPE was calculated to be equal to the total concentration of ABEI molecules on the AuNPs cast on the working electrode based on the starting stock solution used in the synthesis process. Then, ABEI-AuNP/SPE and ABEI-AuNP-GONR/SPE were analyzed in plain CBS buffer without additional ABEI solution. This step was necessary to determine the role of GONR in ECL and demonstrate that ABEI molecules were coated on the AuNPs.

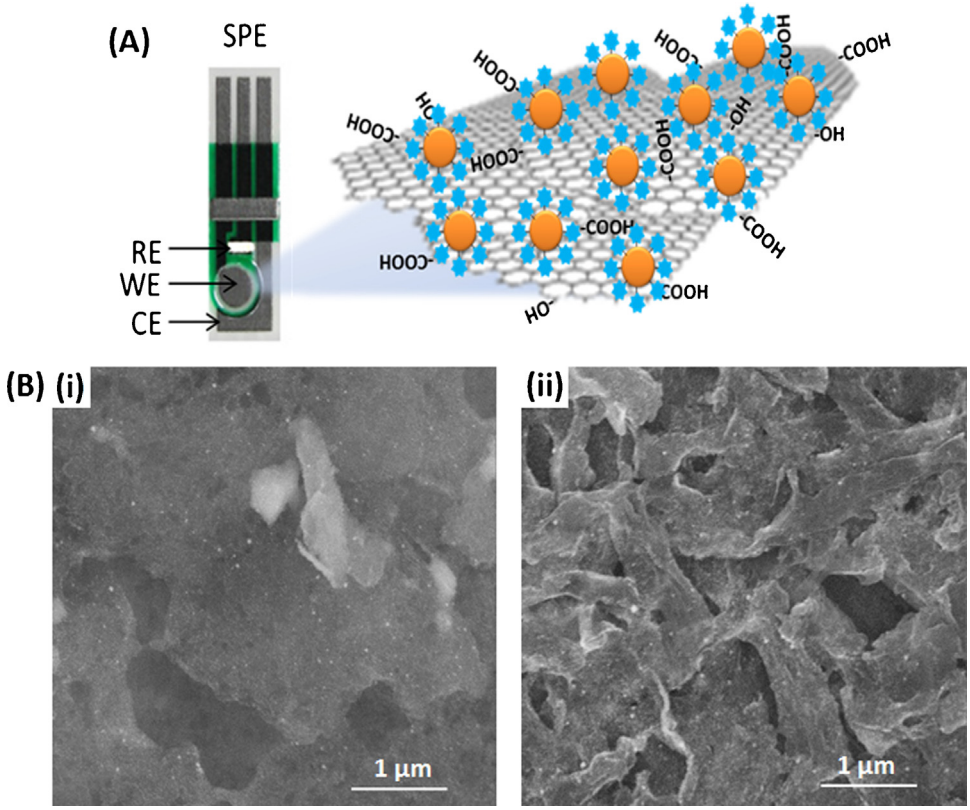

Fig. 1. (A) Illustration of ABEI-AuNP-GONR modified SPE. (B) SEM images of (i) ABEI-AuNP/SPE and (ii) ABEI-AuNP-GONR/SPE electrodes.

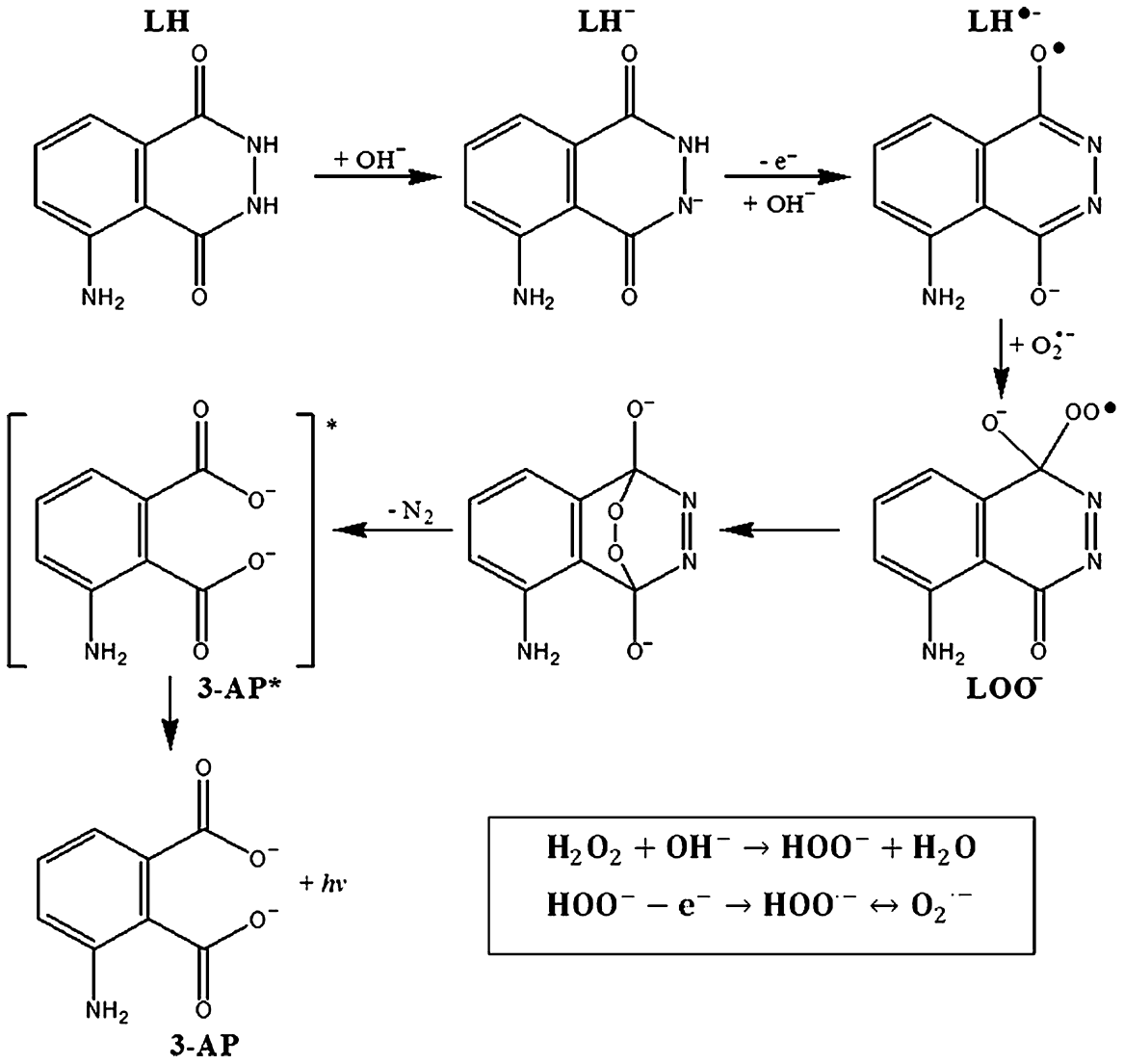

Fig. 2. Basic mechanism of the ECL of luminol under alkaline conditions.

Fig. 3A shows the CV of SPE in ABEI solution, with three oxidation peaks during the forward scan at +0.135, +0.475, and +0.78 V, and one reduction peak at -0.907 V during the reverse scan. The corresponding ECL intensity spectrum in Fig. 3B reveals only two ECL peaks appearing at +0.210 and +0.505 V during the forward scan, while the reverse scan shows two ECL peaks at −0.645 and −0.710 V. To distinguish the mechanism underlying each peak in the CV and ECL intensity spectrum, each component of the solutions used to test the SPE was compared, as depicted in Fig. S4. Based on the previous research on the ECL of luminol on a paraffin-impregnated graphite electrode, the first anodic ECL peak was ascribed to the direct electro-oxidation of luminol to $LH^{\bullet-}$, which consequently produced 3-AP*, thus resulting in the emission of light with or without the presence of dissolved oxygen (O_2) [30]. The second anodic ECL peak was dependent on the first oxidation peak (Fig. S5), which indicated that the $LH^{\bullet-}$ intermediate produced in the first oxidation process was involved in the second oxidation process. The conversion of $LH^{\bullet-}$ to 3-AP* in the second anodic ECL peak may occur by (i) interaction with O_2, (ii) electrochemical oxidation [30], or (iii) oxidation of HOO^- to $O_2^{\bullet-}$, which can subsequently interact with $LH^{\bullet-}$ if H_2O_2 exists in the solution [29]. The CVs in Fig. S4C show an increase in current density in the presence of H_2O_2, corresponding to an increase in the second anodic ECL intensity (Fig. S4D). By comparing to the CVs of the SPE in CBS with and without H_2O_2 in Fig. S4A, we can confirm that the third oxidation peak at +0.78 V was due to the oxidation of H_2O_2 to produce O_2. These results suggest that the oxidation of H_2O_2 to O_2 involves the generation of a $HOO^{\bullet-}$ intermediate that dissociates to $O_2^{\bullet-}$, which subsequently reacts with $LH^{\bullet-}$ and leads to the generation of 3-AP* [29]. We thus conclude that, the second anodic ECL of ABEI on SPE might be due to the simultaneous occurrence reactions (i)-(iii). Finally, the high ECL intensity observed during the reverse scan in the oxygen-reduction region suggested that the O_2 produced during the third oxidation peak was reduced to HOO^- and reacted with the remaining $LH^{\bullet-}$ in the solution to produce 3-AP* [10,15,16,30].

Similar CV and ECL intensity characteristic were observed using GONR/SPE under the same conditions as depicted in Fig. S6. However, the first anodic ECL peak exhibited a positive shift of 35 mV, which could be attributed to the oxygen functional groups on the GONRs limiting the adsorption of ABEI on the electrode surface, thus reducing the ECL intensity (Fig. 3B). In contrast, the oxygen-reduction peak of GONR/SPE shifted negatively by 100 mV relative to SPE; this difference was expectedly because of the contribution of the oxygen functional groups that originally existed

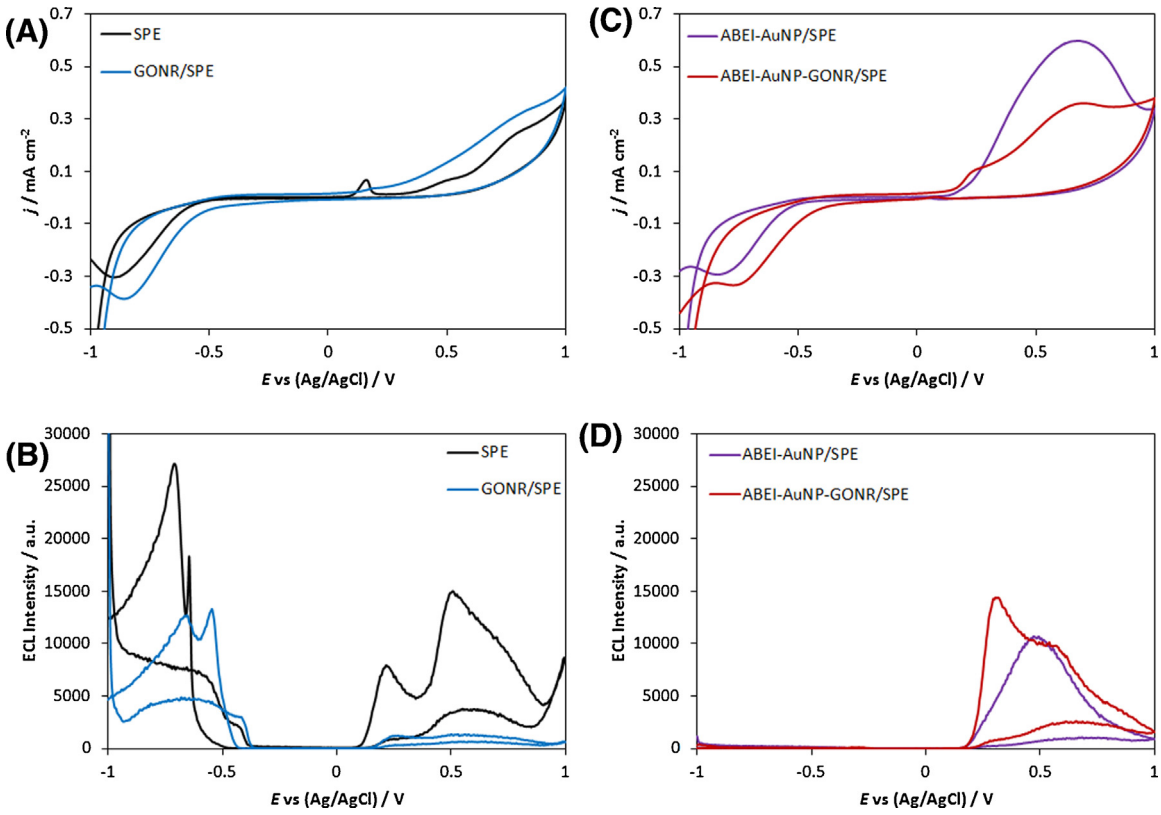

Fig. 3. (A) CVs and (B) ECL intensities of SPE and GONR/SPE in 0.364 mM ABEI solution. (C) CVs and (D) ECL intensities of ABEI-AuNP/SPE and ABEI-AuNP-GONR/SPE. The supporting electrolyte was 1 mM H_2O_2 in 0.02 M CBS (pH 9.85) and the CV scan rate was 50 mV/s.

on GONR to speeding up the reduction process and producing ECL emission.

To confirm the presence of ABEI molecules on the as-prepared ABEI-AuNPs and characterized its ECL activity, the ABEI-AuNP/SPE was tested in blank CBS. Fig. 3C shows that the CV of ABEI-AuNP/SPE only exhibits one oxidation peak at +0.655 V and one reduction peak at −0.824 V. Similar to the CV, the ECL intensity spectrum revealed one anodic ECL peak at +0.470 V, although no cathodic ECL was observed (Fig. 3D). This result confirmed that ABEI molecules exist together with AuNPs and are capable of producing ECL activity. Previous reports on the ECL of luminol solution on Au electrodes under alkaline conditions stated that the oxidation of $LH^{\bullet-}$ by Au hydroxide ($Au(OH)_3$) can yield anodic ECL at 0.5 V [10,15,16]. However, ABEI-AuNP/SPE at the solid-liquid interface cannot generate anodic ECL through the oxidation of $LH^{\bullet-}$ by Au $(OH)_3$ because of the unlikely contact between the Au surface and ABEI molecules. Although we believe that the CV oxidation peak can be ascribed to the formation of gold oxide (Au_2O_3), the anodic ECL might be generated by the interaction of $LH^{\bullet-}$ and $O_2^{\bullet-}$ and the slow subsequent electrochemical oxidation of LH^- and HOO^-. The positive shift in the anodic ECL peak of ABEI-AuNP/SPE relative to that of the SPE in ABEI solution suggested that ABEI-AuNP at the solid-liquid interface has low catalytic activity for the ECL of ABEI. Because luminol oxidation is a rate-determining step in ECL [14], low rates of ABEI oxidation reaction led to poor ECL emission. Moreover, due to the low catalytic activity of ABEI-AuNPs, we believe that the direct electro-oxidation of $LH^{\bullet-}$ to 3-AP* is not possible, unlike in solution-phase ABEI on SPE and GONR/SPE. In the absence of H_2O_2 in the solution, the CV (Fig. S7A) and ECL spectrum (Fig. S7B) showed identical characteristics, but both the oxidation and anodic ECL peaks shifted negatively and exhibited reduced current density and ECL intensity, respectively. The weak anodic ECL might result from the reaction of $LH^{\bullet-}$ with dissolved O_2 [16].

Interestingly, after the integration of the as-prepared ABEI-AuNPs with GONRs to form ABEI-AuNP-GONR/SPE, the CV revealed two oxidation peaks at +0.235 and +0.641 V with one reduction peak at −0.746 V, as shown in Fig. 3C. Similar to the CV, the ECL intensity spectrum also showed two anodic ECL peaks at +0.305 and +0.570 V, although no cathodic ECL peak was observed (Fig. 3D). The CVs of ABEI-AuNP-GONR/SPE in CBS with and without the addition of H_2O_2 (Fig. S7C) exhibit similar characteristic; however, in the presence of H_2O_2, they show positively shifted oxidation potentials and increased current densities. The corresponding ECL spectra demonstrate that the first anodic ECL peak decreased significantly and that the second anodic ECL peak diminished in the absence of H_2O_2 (Fig. S7D). Based on these results, we believed that the first oxidation peak is due to the reaction of LH^- to $LH^{\bullet-}$ that react with $O_2^{\bullet-}$ to form 3-AP*. $O_2^{\bullet-}$ might be generated from the hydroxyl radical ($OH^{\bullet}$) produced when the O-O bond of H_2O_2 was broken by the reaction with HOO^- [14] or from the reaction of $LH^{\bullet-}$ with dissolved O_2 [16]. In contrast, the small shoulder of the second anodic ECL peak might be attributed to the electrochemical oxidation of HOO^- to produce $O_2^{\bullet-}$, which could interact with the remaining $LH^{\bullet-}$ to emit light. The oxidation peak potential of H_2O_2 on ABEI-AuNPs between those of bare Au (0.15 V) and GONR/SPE (0.88 V) electrodes, as shown in Fig. S8(i) and (ii), respectively, appears reasonable. Similar to ABEI-AuNP/SPE, we believe the second oxidation peak of ABEI-AuNP-GONR/SPE was due to the oxidation of Au to Au_2O_3. Compared with ABEI-AuNP/SPE, ABEI-AuNPs supported by GONRs produced a 30.0% improvement in ECL intensity at a much lower potential, suggesting an enhancement in catalytic activity. This catalytic enhancement might attributable to the increase in the AuNP active surface area, which would facilitate oxidative radical

generation and faster reaction kinetics of the ABEI oxidation process. Furthermore, GONRs have been shown to act as a backbone for ABEI-AuNPs and thus prevent aggregation, as observed in Fig. 1B. Moreover, the hybrid of ABEI-AuNPs and GONRs might form a three-dimensional specific non-covalent interaction between the oxygenated functional groups of GONRs and the AuNP active sites, thereby enhancing the catalytic performance of the whole system.

The ECL spectra of solution-phase ABEI on SPE demonstrate high cathodic ECL intensity (Fig. 3B), while the ABEI-AuNP-modified SPE shows no ECL activity during the reverse scan (Fig. 3D). To understand this phenomenon, we used a CCD camera to record the ECL activity on each electrode separately. As shown in Fig. 4A, the SPE in ABEI solution produces high ECL emission at the working electrode during the forward scan while the counter electrode produces ECL emission during the reverse scan. In contrast, ABEI-AuNP/SPE (Fig. 4B) only produces ECL emission at the working electrode during the forward scan. In an electrochemical system, the working electrode behaves as the anode, while the counter electrode behaves as the cathode during the forward scan; the opposite is true during the reverse scan. Thus, the fact that ECL emission only occurred on the anode was demonstrated by the results obtained using solution-phase ABEI on SPE. Because ABEI-AuNPs were only cast on the working electrode of the SPE, no ECL emission was observed during the reverse scan. Up to now, we have predicted a possible ECL mechanism of ABEI-AuNP-GONR/SPE and demonstrated the role of GONRs as a functional supporting matrix in enhancing the catalytic activity and active surface area of ABEI-AuNPs. To achieve better performance of the ABEI-AuNP-GONR/SPE and further confirm the role of GONRs, we optimized the loading ratio between GONRs and ABEI-AuNPs as described in the following section.

3.3. Effect of the loading ratio on ECL of ABEI-AuNP-GONR/SPE

In the previous section, GONRs were shown to be a good supporting matrix for ABEI-AuNPs with regard to catalytic activity enhancement and the prevention of particle aggregation. However, the loading ratio between ABEI-AuNPs and GONRs must be controlled to avoid the aggregation of ABEI-AuNPs at high concentrations and the thick oxygen barrier resulting from the high concentrations of GONR. Therefore, we optimized the ratio of GONR and ABEI-AuNP loadings to achieve the optimal binding between ABEI-AuNPs and the GONR supporting matrix while controlling the size of the AuNPs in the ABEI-AuNP-GONR/SPE. The optimized loading ratio was determined from the maximum measured ECL intensity of the anodic ECL peak in 0.02 M CBS with the addition of 1 mM H_2O_2. Previous studies have shown that high luminol ECL intensity on AuNPs was observed because of the increase AuNP surface area and the greater number of active sites [14]. To demonstrate this relationship, we examined the surface area of each catalytic material coated on SPEs based on the optimum loading ratio of ABEI-AuNP-GONR/SPE in 10 mM ferricyanide at various scan rates. Subsequently, the active surface area was calculated using the Randles-Sevcik equation [18].

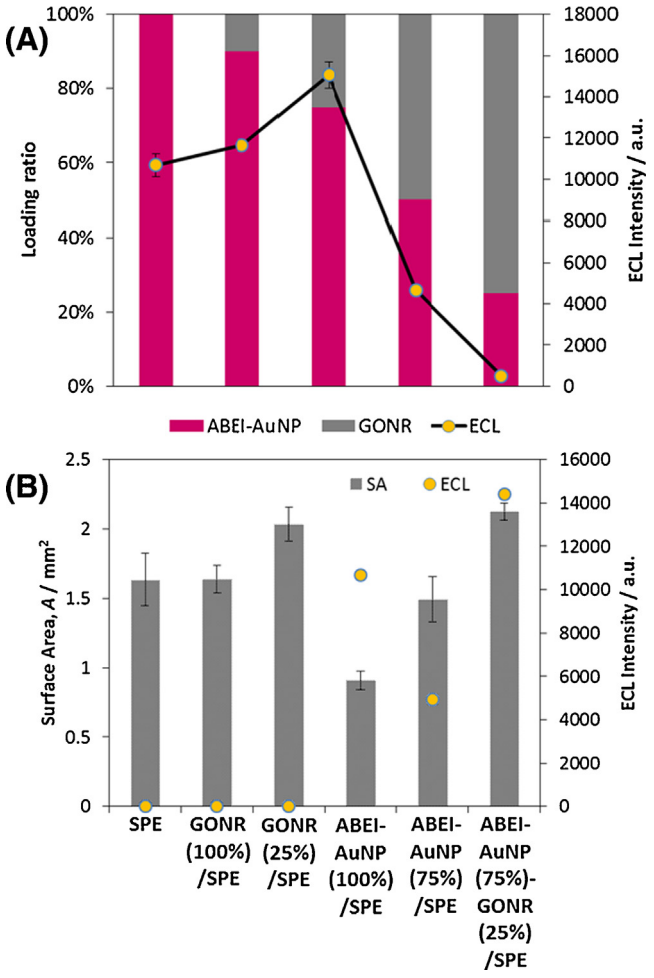

Fig. 5. (A) ECL intensity with various loading ratios of ABEI-AuNPs and GONRs (B) Comparison of anodic ECL peak and calculated active surface area with each tested ratio of catalytic materials. The supporting electrolytes were 1 mM H_2O_2 in 0.02 M CBS (pH 9.85) and 10 mM $K_3[Fe(CN)_6]$ in 1 M KCl for the measurement of ECL intensity and active surface area, respectively.

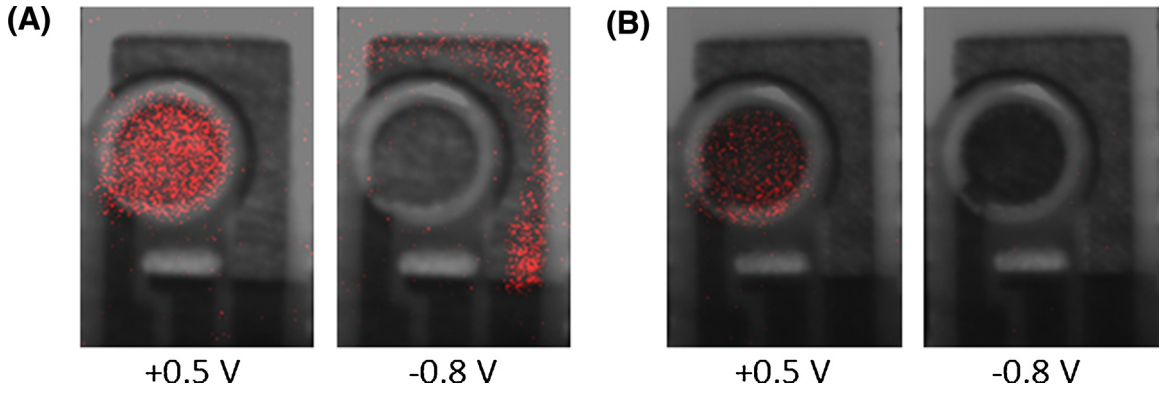

Fig. 4. CCD images of ECL intensity at different potentials on (A) SPE in 0.364 mM ABEI solution and (B) ABEI-AuNP/SPE. The supporting electrolyte was 1 mM H_2O_2 in 0.02 M CBS (pH 9.85) and the CV scan rate was 50 mV/s.

Fig. 5A shows the loading ratio between the as-prepared ABEI-AuNPs and GONRs (1 mg/mL in DI water). The ECL intensity was significantly enhanced by increasing the GONR ratio from 0% to 25% and reducing the proportion of ABEI-AuNPs from 100% to 75%. A further decrease in the ABEI-AuNP loading to 50% with 50% GONRs resulted in strong inhibition of the ECL intensity. The high ECL intensity obtained by using a low loading of GONRs might be due to a smaller extent of ABEI-AuNP aggregation on SPE and the expected increase in the active surface area of the electrode. When a high loading of GONRs and a low loading of ABEI-AuNPs was analyzed, the reduction in the ECL intensity was found to result primarily from the small amounts of ABEI on the electrode. Additionally, a high loading of GONR led to a large quantity of oxygen functional groups being present on the electrode. These functional groups form an oxide layer that acts as a barrier in the electron-transfer process, and thus lowers the oxidation rates of ABEI [6]. Based on these experiments, a loading ratio of 75% ABEI-AuNPs to 25% GONRs was chosen as the optimum loading ratio for further experiments.

Based on the optimum loading ratio of ABEI-AuNP-GONR/SPE, the contributions of each catalytic material toward the active surface area and ECL intensity were compared. Fig. 5B shows the increase in the active surface area resulting from the modification of the SPE electrode with GONRs. The four-fold dilution of a solution corresponding to 100% GONR loading (2 μL of 1 mg/mL) in water before casting led to a 21.7% increase in the active surface area. This phenomenon might be related to improvements in electron transfer by decreasing the number of oxide ions insulating the electrode surface. In the case of ABEI-AuNPs, a 25% loading reduction in the as-prepared ABEI-AuNPs used to modify the SPE led to a 48.8% increase in the active surface area but a 53.7% decrease in the ECL intensity. This result suggests that a higher loading of ABEI-AuNPs promotes large amounts of aggregation on the electrode surface. Lowering the loading of ABEI-AuNPs is thus expected to reduce the ECL intensity by decreasing the amount of ABEI molecules on the electrode. Interestingly, using 25% GONRs and 75% ABEI-AuNPs led to increases of 34.9% and 97.8% in the total active surface area and ECL intensity, respectively. Therefore, we confirmed that GONRs play a very important role as a functional supporting matrix in enhancing the catalytic activity of ABEI-AuNPs in the ECL reaction, and also act as a backbone to prevent the aggregation of AuNPs. The high catalytic activity of ABEI-AuNPs might have led to the active generation of oxidative radicals, which subsequently enhanced the ECL intensity. The following section will discuss the influences of buffer pH and the existence of H_2O_2 and dissolved O_2 on the ECL reaction to further clarify the mechanism of ABEI-AuNP at the solid-liquid interface.

3.4. Effect of pH, H_2O_2 concentration and dissolved O_2 on the ECL of ABEI-AuNP-GONR/SPE

The effect of pH on the ECL of ABEI-AuNP-GONR/SPE was determined using CBS with pH values ranging from 9.02 to 10.72, as shown in Fig. 6. The ECL intensity increased significantly as the pH value increased and was maximized at pH 10.02. The enormous increase in the ECL intensity achieved with the addition of 1 mM H_2O_2 as the pH value increased might suggest enhancements in the generation of oxidative species, such as $OH^{\bullet}$ and $O_2^{\bullet-}$, which are necessary in the conversion of $LH^{\bullet-}$ to 3-AP* [10]. Furthermore, the presence of the ABEI-AuNP catalyst facilitated the epoxidation of H_2O_2 reaction via O-O bond on the Au surface. AuNP catalysis might break the O-O bond to form $OH^{\bullet}$, which subsequently interacts with HOO^- to form $O_2^{\bullet-}$ [14]. In addition, a basic solution is also important in preparing the LH^- and HOO^- precursors for further electrochemical oxidization to produce $LH^{\bullet-}$ and $O_2^{\bullet-}$ radicals. However, at very high pH values, a decrease in the ECL intensity was observed, which might be due to the formation of substantial amount of hydroxide ions (OH^-) on the electrode surface, which could interfere with H_2O_2 dissociation on the AuNP surface, and thereby hinder the generation of $O_2^{\bullet-}$. In the case of ABEI-AuNP-GONR/SPE tested in CBS with various pH values of in the absence of H_2O_2, the ECL intensity exhibits only a small increase because ECL is mainly generated through the interaction between $LH^{\bullet-}$ and dissolved O_2 to produce 3-AP*. Similarly, CV of ABEI-AuNP-GONR/SPE under neutral conditions (Fig. S9) shows that the ABEI oxidation reaction begins at 0.48 V and produces very low ECL intensity and that the peak shifts positively by 150 mV relative to that of ABEI-AuNP-GONR/SPE tested under alkaline conditions. These results indicate that neutral pH provides an insufficient amount of oxidative radicals to produce appreciable amounts of $O_2^{\bullet-}$, thus slowing the ABEI oxidation reaction to form $LH^{\bullet-}$ and consequently leading to a low rate of 3-AP* [5]. Thus, we have demonstrated that the generation of $O_2^{\bullet-}$ in the presence of H_2O_2 is important for the production of intense ECL emission.

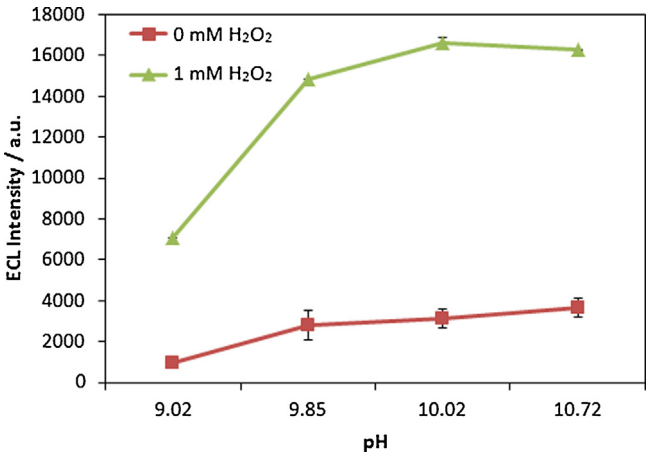

Fig. 6. ECL intensity of ABEI-AuNP-GONR/SPE in relation to the pH of the buffer solution in the presence and absence of 1 mM H_2O_2.

H_2O_2 plays an important role in the ECL of luminol by facilitating the formation of the oxidative radicals needed to produce the 3-AP* excited state, as discussed in the previous section. Fig. 7A shows that the ECL intensity increases significantly as the concentration of H_2O_2 increases, and the second ECL peak thus becomes more obvious. Moreover, the ECL peak intensity shifts positively with increasing H_2O_2 concentration. The results presented above suggest that H_2O_2 facilitates the generation of $O_2^{\bullet-}$ radicals through the oxidation of HOO^- and also simultaneously contributes to $OH^{\bullet}$ formation on the ABEI-AuNP surface by epoxidation. However, this process creates competition between radicals to absorb on the electrode surface, resulting in positively shifted anodic ECL peaks. When low concentrations of H_2O_2 were used, most of the HOO^- formed $O_2^{\bullet-}$ radicals by reacting with $OH^{\bullet}$, which was consumed to generate the first ECL peak with $LH^{\bullet-}$. We can assume that the HOO^- concentration involved in the second ECL peak increases as the H_2O_2 concentration increases through the electrochemical oxidization of the remaining HOO^- to $O_2^{\bullet-}$ and its subsequent reaction with $LH^{\bullet-}$ to generate 3-AP* for the second anodic ECL peak. However, we also can observe high ECL intensity without the addition of H_2O_2. This phenomenon might suggest that the ECL of ABEI can result from the reaction of $LH^{\bullet-}$ with dissolved O_2 under basic conditions. Therefore, ABEI-AuNP-GONR/SPE was thoroughly investigated in deaerated CBS, which was purged with nitrogen gas (N_2) for 30 min before the experiment. Fig. 7B shows that the ECL intensity increases as the H_2O_2 concentration increases in deaerated CBS. However, the recorded ECL intensity was lower than that in normal CBS containing dissolved O_2. This

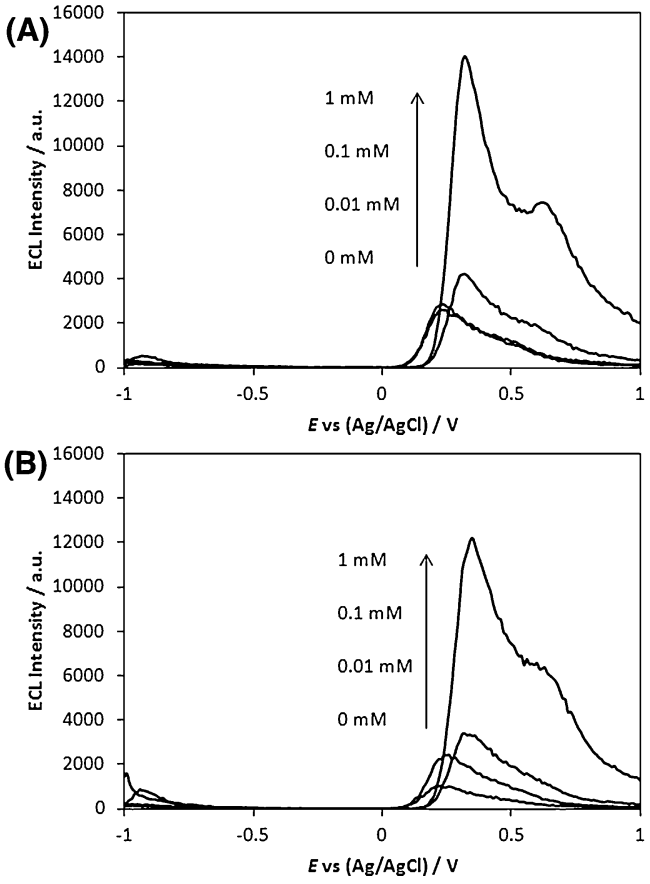

Fig. 7. ECL intensity of ABEI-AuNP-GONR/SPE in (A) CBS and (B) deaerated CBS (pH 9.85) with various concentrations of H_2O_2. The scan rate was 100 mV/s.

result further confirms that dissolved O_2 makes a minor contribution to the generation of $O_2^{\bullet-}$ through $LH^{\bullet-}$ for ECL emission. Moreover, ECL intensity can be detected on ABEI-AuNP-GONR/SPE in deaerated CBS without the addition of H_2O_2. This result indicates that $LH^{\bullet-}$ can be converted into 3-AP* through direct electro-oxidation in the absence of O_2 and HOO^- [10]. In the absence of dissolved O_2, the second ECL peak was not observed at low concentrations of H_2O_2. Thus, we conclude that the pH of the buffer and the concentrations of H_2O_2 and dissolved O_2 contribute to the formation of oxidative radicals, mainly $O_2^{\bullet-}$, which is a strong co-oxidant of $LH^{\bullet-}$ for ECL. In addition, the generation of radicals also depends on the ABEI-AuNP catalysis, which was significantly enhanced by the use of GONRs as a supporting matrix. The possible mechanism of ABEI-AuNP-GONR/SPE in generating ECL on ABEI-AuNP-GONR/SPE is described in the next section.

3.5. Proposed ECL mechanism of ABEI-AuNP-GONR/SPE

The ECL of ABEI-AuNP-GONR/SPE exhibited two anodic ECL peaks. The experimental results demonstrate that the first anodic ECL peak is highly dependent on pH, H_2O_2 concentration, and ABEI-AuNP catalysis. Analyzing ABEI-AuNP-GONR/SPE ECL under a nitrogen atmosphere without the addition H_2O_2 revealed weak ECL, demonstrating that $LH^{\bullet-}$ can undergo direct electro-oxidation to 3-AP* in the absence of $O_2^{\bullet-}$, as shown in Eq. (1). Otherwise, $LH^{\bullet-}$ is expected to interact with $O_2^{\bullet-}$ to produce 3-AP*, as shown in Eq. (4)–(6). The generation of $O_2^{\bullet-}$ may occur via either the interaction of HOO^- with $OH^{\bullet}$ resulting from H_2O_2 epoxidation with ABEI-AuNP catalysis, as shown in Eq. (2), or the direct reaction of $LH^{\bullet-}$ with the dissolved O_2 that naturally exists in the solution, as shown in Eq. (3).

$$LH^- - e^- \rightarrow LH^{\bullet-} + H^+ \quad (1)$$

$$HOO^- + OH^{\bullet} \rightarrow O_2^{\bullet-} + H_2O \quad (2)$$

$$LH^{\bullet-} + O_2 \rightarrow O_2^{\bullet-} + L \quad (3)$$

$$LH^{\bullet-} + O_2^{\bullet-} \rightarrow LOO^- \quad (4)$$

$$LOO^- \rightarrow 3-AP^* + N_2 \quad (5)$$

$$3-AP^* \rightarrow 3-AP + h\nu \quad (6)$$

In contrast, the second anodic ECL is mainly dependent on high concentration of H_2O_2, as was confirmed in both deaerated and non-deaerated CBS. The emission of light was predicted to be the

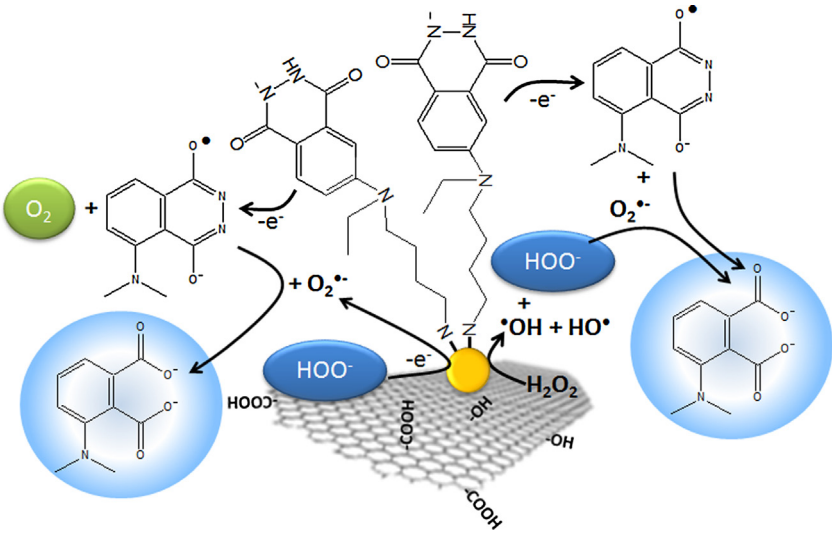

Fig. 8. Illustration of the proposed ECL mechanism of ABEI-AuNP-GONR/SPE.

result of the interaction between $LH^{\bullet -}$ and $O_2^{\bullet -}$, which was produced through the electrochemical oxidation of HOO^-. The overall ECL mechanism of ABEI-AuNP-GONR/SPE under alkaline conditions with the addition of H_2O_2 can be illustrated as in Fig. 8.

$$HOO^- - e^- \rightarrow HOO^{\bullet -} \leftrightarrow O_2^{\bullet -} \quad (7)$$

$$LH^{\bullet -} + O_2^{\bullet -} \rightarrow LOO^- \quad (4)$$

$$LOO^- \rightarrow 3 - AP^* + N_2 \quad (5)$$

$$3 - AP^* \rightarrow 3 - AP + h\nu \quad (6)$$

3.6. Characterization of the interaction between ABEI-AuNPs and GONRs

To further clarify the interaction between ABEI-AuNPs and GONRs, ATR-FTIR spectra of each catalytic material were obtained. We prepared 1 mL solutions of GONRs and ABEI-AuNPs in DI water based on the ratio used for the ABEI-AuNP-GONR mixture. These solutions were centrifuged to remove the DI water. Then, 0.5 mL of ethanol was added, and the mixture was sonicated to produce a well-dispersed catalyst solution. Immediately after that, a small amount of catalyst was casted onto the ATR diamond surface to form a thin layer. The FTIR spectra in Fig. 9 show common peaks at 2300 cm^{-1}, which are attributed to the asymmetric stretching vibration of CO_2, while the noise signals in the 3400–4000 cm^{-1} and 1300–1900 cm^{-1} regions are ascribed to water vapor [31]. Apart from those signals, the GONR spectrum showed a strong hydroxyl band at approximately 3200 cm^{-1} (i) of COO–H/O–H stretching, in addition to four carbonyl bands at around 1700 cm^{-1} (iii), which corresponded to C=O stretching; around 1564 cm^{-1} (iv), attributed to –COO– asymmetric stretching; around 1030 cm^{-1} (vii), corresponding to C–O stretching; and around 1209 cm^{-1} (viii), resulting from O–H deformation [18,31].

The appearance of hydroxyl and carbonyl bands indicates that the GONRs had successfully undergone the oxidative unzipping process. In comparison, the ABEI-AuNP spectrum revealed a broad peak at 3400 cm^{-1}, signifying a weak covalent interaction between the amino group in ABEI and the AuNPs [24]. Moreover, the ABEI-AuNP spectrum shows strong aromatic C=C bending at 1500 cm^{-1} (v) with two alkane bands at around 2900 cm^{-1} (ii), attributed to C–H stretching, and around 1390 cm^{-1} (vi), corresponding to C–H deformation. Interestingly, the ABEI-AuNP-GONR mixture showed a decrease in the absorbance intensities of the hydroxyl and carbonyl bands of the GONRs, indicating that the ABEI-AuNPs exhibited metal-oxygen bonding with GONRs that enhanced the catalytic performance [28,31]. In addition, the disappearance of the aromatic band of ABEI-AuNPs after mixing with GONRs might suggest non-covalent interactions between the benzene ring of ABEI and the benzene domain of the GONRs.

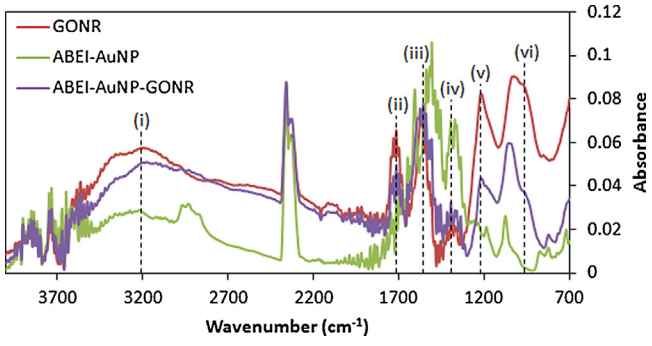

Fig. 9. ATR-FTIR spectra of the ABEI-AuNP and GONR precursors used to form the ABEI-AuNP-GONR mixture.

4. Conclusions

In summary, we have synthesized and optimized a hybrid of ABEI-AuNPs with GONRs through simple mixing and deposition on a carbon SPE. The catalytic activity of ABEI-AuNP-GONR/SPE for the ECL of ABEI has been studied and compared to that of ABEI-AuNP/SPE under alkaline conditions. The intercalation of ABEI-AuNPs with GONRs resulted in a 30.0% increase in the ECL intensity resulting from an 80.2% increase in the active surface area compared with ABEI-AuNP/SPE. In addition, CVs revealed that ABEI-AuNPs without the support of GONRs show slow reaction kinetics towards ABEI oxidation but produce 50.1% higher peak current density. These results suggest that the high ECL emission from ABEI-AuNP-GONR/SPE might be due to the interaction between electrochemically generated luminol radicals and oxidative radicals, which were independently generated through ABEI-AuNP catalysis. Consequently, GONRs have been identified to act as a backbone with ABEI-AuNPs to prevent aggregation through non-covalent interactions and metal-oxygen bonding between the oxygen functional groups of GONR with the ABEI-AuNP active sites, thereby enhancing the catalytic performance of the whole system. Further work to utilize ABEI-AuNP-GONR/SPE in an enzyme-based ECL sensor is being undertaken in our laboratory, which will pave the way for future developments of rapid and portable point-of-care device.

Acknowledgement

We would like to thank Dr. Vu Thi Huong, Dr Tomohiko Ikeuchi, Akiko Araki, Takuma Horii, and Daiki Mita for technical support. We thank Dr Mukhzeer Mohamad Shahimin for helpful input to improve this manuscript.

Appendix A. Supplementary data

Supplementary data associated with this article can be found, in the online version, at http://dx.doi.org/10.1016/j.electacta.2015.08.043.

References

[1] M.M. Richter, Electrochemiluminescence (ECL), Chem. Rev. 104 (2004) 3003.
[2] Y. Su, Y. Lv, Graphene and graphene oxide: recent advances in chemiluminescence and electrochemiluminescence, R. Soc. Chem. Adv. 4 (2014) 29324.
[3] A.J. Bard, Electrogenerated Chemiluminescence, Marcel Dekker, Inc., New York, 2004.
[4] G. Merényi, J. Lind, T.E. Eriksen, Luminol chemiluminescence: chemistry, excitation, emitter, J. Biolumin. Chemilumin. 5 (1990) 53.
[5] G. Merényi, J.S. Lind, Role of peroxide intermediate in the chemiluminescence of luminol. A mechanistic study, J. Am. Chem. Soc. 102 (1980) 5830.
[6] S. Sakura, Electrochemiluminescence of hydrogen peroxide-luminol at a carbon electrode, Anal. Chim. Acta 262 (1992) 49.
[7] P.M. Easton, A.C. Simmonds, A. Rakishev, A.M. Egorov, L.P. Candeias, Quantitative model of the enhancement of peroxidase-induced luminol luminescence, J. Am. Chem. Soc. 118 (1996) 6619.
[8] A.N. Diaz, F.G. Sanchez, J.A.G. Garcia, Hydrogen peroxide assay by using enhanced chemiluminescence of the luminol-H_2O_2-horseradish peroxidase system: comparative studies, Anal. Chim. Acta 327 (1996) 161.
[9] S. Sakura, H. Imai, Determination of sub-nmol hydrogen peroxide by electrochemiluminescence of luminol in aqueous solution, Anal. Sci. 4 (1988) 9.
[10] H. Cui, Z.F. Zhang, G.Z. Zou, X.Q. Lin, Potential-dependent electrochemiluminescence of luminol in alkaline solution at a gold electrode, J. Electroanal. Chem. 566 (2004) 305.

[11] X. Chen, B. Su, X. Song, Q. Chen, X. Chen, X. Wang, Recent advances in electrochemiluminescent enzyme biosensors, Trends Anal. Chem. 30 (2011) 665.
[12] G.P. Jirka, A.F. Martin, T.A. Nieman, pH and concentration response surfaces for the luminol-H_2O_2 electrogenerated chemiluminescence reaction, Anal. Chim. Acta 284 (1993) 345.
[13] D. Strmcnik, K. Kodama, D. van der Vliet, J. Greeley, V.R. Stamenkovic, N.M. Markovic, The role of non-covalent interactions in electrocatalytic fuel-cell reactions on platinum, Nat. Chem. 1 (2009) 466.
[14] Z.F. Zhang, H. Cui, C.Z. Lai, L.J. Liu, Gold nanoparticle-catalyzed luminol chemiluminescence and its analytical application, Anal. Chem. 77 (2005) 3324.
[15] Y.P. Dong, H. Cui, Y. Xu, Comparative studies on electrogenerated chemiluminescence of luminol on gold nanoparticle modified electrodes, Langmuir 23 (2007) 523.
[16] H. Cui, Y. Xu, Z.F. Zhang, Multichannel electrochemiluminescence of luminol in neutral and alkaline aqueous solutions on a gold nanoparticle self-assembled electrode, Anal. Chem. 76 (2004) 4002.
[17] H. Cui, W. Wang, C.F. Duan, Y.P. Dong, J.Z. Guo, Synthesis, characterization, and electrochemiluminescence of luminol-reduced gold nanoparticles and their application in a hydrogen peroxide sensor, Chem. Eur. J. 13 (2007) 6975.
[18] N.S. Ismail, Q.H. Le, H. Yoshikawa, M. Saito, E. Tamiya, Development of non-enzymatic electrochemical glucose sensor based on graphene oxide nanoribbon-gold nanoparticle hybrid, Electrochim. Acta 146 (2014) 98.
[19] A.K. Geim, K.S. Novoselov, The rise of graphene, Nat. Mater. 6 (2007) 183.
[20] D.V. Kosynkin, A.L. Higginbotham, A. Sinitskii, J.R. Lomeda, A. Dimiev, B.K. Price, J.M. Tour, Longitudinal unzipping of carbon nanotunes to form graphene nanoribbons, Nature 458 (2009) 872.
[21] A.L. Hogginbotham, D.V. Kosynkin, A. Sinitskii, Z. Sun, J.M. Tour, Lower-defect graphene oxide nanoribbons from multiwalled carbon nanotubes, ACS Nano 4 (2010) 2059.
[22] K. Idegami, M. Chikae, N. Nagatani, E. Tamiya, Y. Takamura, Fabrication and characterization of planar screen-printed Ag/AgCl reference electrode for disposable sensor strip, Jpn. J. Appl. Phys. 49 (2010) 097003.
[23] D. Tian, H. Zhang, Y. Chai, H. Cui, Synthesis of *N*-(aminobutyl)-*N*-(ethylisoluminol) functionalized gold nanomaterials for chemiluminescence for chemiluminescence bio-probe, Chem. Commun. 47 (2011) 4959.
[24] W. Shen, D. Tian, H. Cui, D. Yang, Z. Bian, Nanoparticle-based electrochemiluminescence immunosensor with enhanced sensitivity for cardiac troponin I using *N*-(aminobutyl)-*N*-(ethylisoluminol) functionalized gold nanoparticles as labels, Biosens. Bioelectron. 27 (2011) 18.
[25] W. Wang, T. Xiong, H. Cui, Fluorescence and electrochemiluminescence of luminol-reduced gold nanoparticles: photostability and platform effect, Langmuir 24 (2008) 2826.
[26] http://www.biodevicetech.com/products/depchip/dep_ep.shtml (accessed January 2014).
[27] http://www.biodevicetech.com/BDTminiSTATleaf100707.pdf , (accessed January 2014).
[28] G. Goncalves, P.A.A.P. Marques, C.M. Granadeiro, H.I.S. Nogueira, M.K. Singh, J. Grácio, Surface modification of graphene nanosheets with gold nanoparticles: the role of oxygen moieties at graphene surface on gold nucleation and growth, Chem. Mater. 21 (2009) 4796.
[29] K.E. Haapakka, J.J. Kankare, The mechanism of the electrogenerated chemiluminescence of luminol in aqueous alkaline solution, Anal. Chim. Acta 138 (1982) 263.
[30] H. Cui, G.Z. Zou, X.Q. Lin, Electrochemiluminescence of luminol in alkaline solution at a paraffin-impregnated graphite electrode, Anal. Chem. 75 (2003) 324.
[31] L.Q. Hoa, M.C. Vestergaard, H. Yoshikawa, M. Saito, E. Tamiya, Enhancing catalytic performance of Pt-based electrode with a noncovalent interaction-induced functionalized carbon nanotube-grafted matrix, J. Mater. Chem. 22 (2012) 14705.